

EPR observations of trivalent titanium in orthophosphate single crystals

M. M. Abraham, L. A. Boatner, and M. A. Aronson

Citation: *J. Chem. Phys.* **85**, 1 (1986); doi: 10.1063/1.451638

View online: <http://dx.doi.org/10.1063/1.451638>

View Table of Contents: <http://jcp.aip.org/resource/1/JCPSA6/v85/i1>

Published by the AIP Publishing LLC.

Additional information on J. Chem. Phys.

Journal Homepage: <http://jcp.aip.org/>

Journal Information: http://jcp.aip.org/about/about_the_journal

Top downloads: http://jcp.aip.org/features/most_downloaded

Information for Authors: <http://jcp.aip.org/authors>

ADVERTISEMENT

physicstoday

**Comment on any
Physics Today article.**

The advertisement shows a red arrow pointing from the text to a sample comment on a *Physics Today* article. The article title is "Measured energy in Japan" by David von Seggern. The comment, written by Edgar McCarroll on July 14, 2012, discusses the energy released by a 100-megaton explosion and compares it to the energy released by a 100-megaton nuclear bomb. The comment also mentions the 1964 Chilean earthquake and the 1964 nuclear device.

EPR observations of trivalent titanium in orthophosphate single crystals^{a)}

M. M. Abraham, L. A. Boatner, and M. A. Aronson

Solid State Division, Oak Ridge National Laboratory, Oak Ridge, Tennessee 37831

(Received 6 January 1986; accepted 21 March 1986)

The ground state spectroscopic properties of the $3d^1$ electronic configuration ion Ti^{3+} have been investigated using EPR spectroscopy. Trivalent titanium was incorporated as a dilute impurity in single crystals of the tetragonal, zircon-structure hosts $ScPO_4$, YPO_4 , and $LuPO_4$. The EPR spectrum of Ti^{3+} was observed in the as-grown orthophosphate crystals, and low temperature irradiations were not required to produce the trivalent state. The EPR results show that Ti^{3+} occupies a substitutional cation site in the host orthophosphate single crystals. Axial spin-Hamiltonian parameters were determined at 77 K, and these results are compared to those obtained previously for the $4d^1$ and $5d^1$ configuration ions Zr^{3+} and Hf^{3+} in the same host crystals. Titanium-doped orthophosphate crystals containing isotopically enriched ^{47}Ti or ^{49}Ti were also grown and employed in determinations of the hyperfine parameters. The g -values observed here for Ti^{3+} , and determined previously for Zr^{3+} and Hf^{3+} are not accounted for by the published second-order expressions indicating that additional coupling mechanisms are operative.

INTRODUCTION

The solid state chemical and physical properties of the lanthanide orthophosphates have been extensively investigated as part of an in-depth evaluation of the applicability of phosphate ceramics to the disposal of high-level nuclear wastes.¹⁻³ Previous investigations of both single crystal and polycrystalline rare-earth orthophosphates have included studies employing EPR spectroscopy,⁴⁻¹² x-ray diffraction,¹³⁻¹⁵ optical absorption and Raman spectroscopy,¹⁶⁻²⁰ and Rutherford backscattering.²¹

At elevated temperatures, the lanthanide orthophosphates crystallize with two different structural types depending on the position of the lanthanide in the transition series. Orthophosphates of the first-half of the series (i.e., $LaPO_4$ to $GdPO_4$) crystallize in the monoclinic "monazite" structural form. The results of previous EPR studies⁵ show that, in the monoclinic monazite unit cell, there are four different lanthanide sites that can be effectively reduced to two different pairs of magnetically equivalent sites as a result of symmetry. (The local crystalline electric field is identical at the four lanthanide positions, but the crystal-field axes are symmetry related in such a manner that, in a magnetic resonance experiment, two sets of magnetically inequivalent spectra are observed at an arbitrary applied magnetic-field orientation.)

Orthophosphates of the second-half of the series (i.e., $TbPO_4$ to $LuPO_4$ as well as YPO_4 and $ScPO_4$) crystallize in a tetragonal structure. This tetragonal structural form is an analog of the minerals zircon $ZrSiO_4$ and xenotime YPO_4 . In the case of the tetragonal zircon-structure orthophosphates, all of the lanthanide sites are magnetically equivalent, and, thus, only one EPR spectrum is observed at any given magnetic-field orientation. This reduced complexity greatly simplifies the interpretation of EPR spectra for impurities in the

tetragonal-symmetry orthophosphate hosts. For this reason, the diamagnetic tetragonal hosts $ScPO_4$, YPO_4 , and $LuPO_4$ have been employed in most previous EPR studies of iron group, rare-earth, actinide, and other paramagnetic species. In particular, recent observations of the unusual trivalent state of Zr were accomplished using these tetragonal hosts,¹¹ and an unequivocal confirmation of the identification of the Zr^{3+} EPR resonance was achieved by using isotopically enriched (to $\approx 95\%$) zirconium-91 (the natural abundance of ^{91}Zr is $\approx 11\%$).

The observation of the unusual trivalent state associated with a $4d^1$ electronic configuration for Zr—an element that is generally found in the tetravalent state—led to attempts to incorporate other ions associated with unusual valence states into $ScPO_4$, YPO_4 , and $LuPO_4$ single crystals. By employing ionizing radiation at low temperature, substitutional trivalent hafnium ions ($5d^1$ electronic configuration) were also observed in the three hafnium doped host crystals $ScPO_4$, YPO_4 , and $LuPO_4$.¹² Upon warming to room temperature, the trivalent hafnium reverted to its original, normally observed, diamagnetic tetravalent state. In the present work, we report the observation by EPR of trivalent titanium ($3d^1$) ions incorporated in single crystals of $ScPO_4$, YPO_4 , and $LuPO_4$. Unequivocal identification of trivalent titanium occupying substitutional metal sites was made by employing special isotopically enriched samples of titanium. Principal axial spectroscopic splitting factors and hyperfine parameters were determined for Ti^{3+} in these hosts and compared with similar data obtained previously for Zr^{3+} and Hf^{3+} .

EXPERIMENTAL

Titanium doped single crystals of $ScPO_4$, YPO_4 , and $LuPO_4$ were grown by first reacting the appropriate host and titanium oxides with lead hydrogen phosphate at 1360 °C. Excess $PbHPO_4$ decomposed to form a $Pb_2P_2O_7$ flux, and the crystal growth process was carried out in a manner described previously.¹² Unequivocal identification of the mag-

^{a)} Research sponsored by the Division of Materials Sciences, U.S. Department of Energy under Contract No. DE-AC05-84OR21400 with Martin Marietta Energy Systems, Inc.

netic resonance of Ti^{3+} depends on the observation of a characteristic hyperfine spectrum consistent with the known abundance of the two odd titanium isotopes. Since the natural abundance of ^{47}Ti and ^{49}Ti is only 7.28% and 5.51%, respectively, isotopically enriched samples were prepared. Three isotopically enriched samples of Ti in the form of TiO_2 were obtained from the ORNL Isotope Sales Department. Two different samples of enriched ^{49}Ti were employed with one having an abundance of 76.27% for ^{49}Ti and 1.67% for ^{47}Ti and the second a ^{49}Ti abundance of 96.25% and a ^{47}Ti abundance of 0.22%. The third enriched sample contained isotopic abundances of 94.55% for the ^{47}Ti isotope and 0.19% for the ^{49}Ti isotope. EPR investigations of the titanium-doped orthophosphate single crystals were carried out in the temperature range between 77 K and room temperature using a conventional X-band spectrometer which employed a Varian TE₁₀₂ mode cavity with 100 KHz modulation frequency. A proton magnetic resonance probe was used to measure the applied magnetic field, and both the microwave and proton resonance frequencies were determined using a Hewlett-Packard HP-5245L frequency counter with an HP-5255A frequency converter. The samples could be rotated through 360° about a vertical axis and tilted several degrees about a horizontal axis allowing accurate alignment of the principal axes of the sample with the magnetic field.

RESULTS AND DISCUSSION

Crystals of LuPO_4 doped with enriched ^{49}Ti (76.27% ^{49}Ti , 1.67% ^{47}Ti , 22.06% ^{47}Ti) were examined. An intense

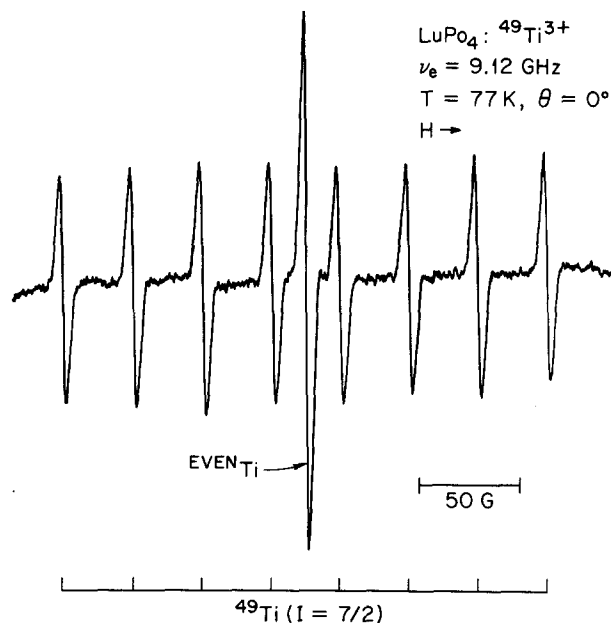


FIG. 1. EPR spectrum of isotopically enriched Ti^{3+} at 77 K in a single crystal of LuPO_4 with the applied magnetic field parallel to the fourfold symmetry axis of the tetragonal crystal. The 76.27% abundance of ^{49}Ti increases the intensity of the eight ^{49}Ti lines relative to the six ^{47}Ti lines and the central ^{47}Ti ($I = 0$) line. The absorption lines (shown in a first derivative presentation) are labeled by the bar diagram below the spectrum.

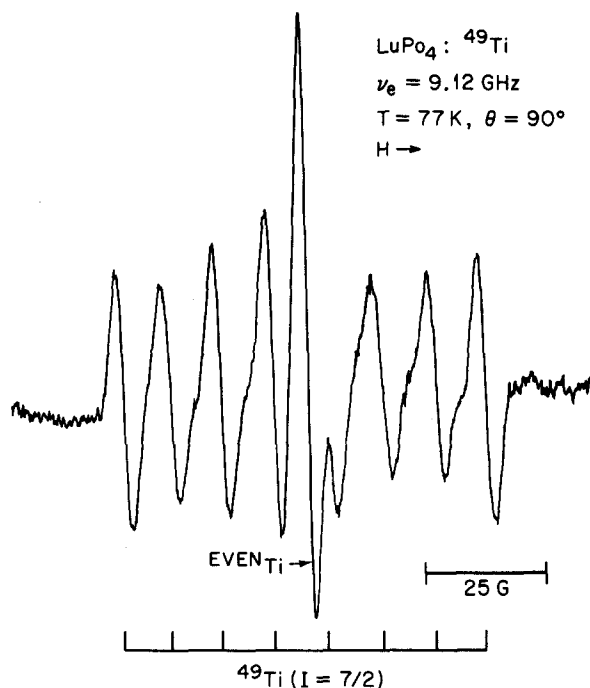


FIG. 2. EPR spectrum (first derivative of absorption vs applied magnetic field) of isotopically enriched Ti^{3+} (enriched to 76.27% ^{49}Ti) at 77 K with the applied magnetic field perpendicular to the fourfold symmetry axis of the LuPO_4 host crystal.

EPR spectrum due to Ti^{3+} was observed in the as-grown LuPO_4 crystals, and it was not necessary to perform a low-temperature irradiation to produce the trivalent state. The increased intensity of the eight hyperfine structure lines for the enriched ^{49}Ti isotope ($I = 7/2$) definitely identified the titanium EPR spectrum. By varying the crystal orientation with respect to the external magnetic field, it was established that the trivalent titanium is located substitutionally in a lutetium site and that the magnetic axes of the paramagnetic ion are coincident with the crystallographic axes of the tetragonal LuPO_4 host. The EPR spectrum obtained at 77 K with the crystallographic c -axis parallel to the external magnetic field is presented in Fig. 1, while in Fig. 2 the corresponding spectrum obtained with the c axis perpendicular to the external field is shown. The spectroscopic parameters g_{\parallel} , g_{\perp} , $^{49}A_{\parallel}$, and $^{49}A_{\perp}$ were obtained by fitting the usual axially symmetric spin Hamiltonian

$$\mathcal{H} = \mu_B \mathbf{H} \cdot \mathbf{g} \cdot \mathbf{S} + A_{\parallel} I_z S_z + A_{\perp} (I_x S_x + I_y S_y) \quad (1)$$

with $S = 1/2$, and these values are listed in Tables I and II.

Single crystals of Ti-doped ScPO_4 were also grown using the 76.27% enriched ^{49}Ti sample as a dopant. In Figs. 3 and 4, the EPR spectrum obtained at 77 K from this Ti-doped ScPO_4 crystal is shown with the applied magnetic field, respectively, parallel and perpendicular to the crystalline c axis. Again, the clear resolution of the eight hyperfine lines due to the enriched ^{49}Ti ($I = 7/2$) isotope provides a positive identification of the titanium spectrum. The ^{47}Ti ($I = 0$) EPR line can be seen near the center of the eight-line hyperfine pattern in Figs. 3 and 4. The transitions are labeled by the bar diagram at the bottom of the figures. Additional

TABLE I. Spin Hamiltonian parameters at 77 K.

	Host	g_{\parallel}	g_{\perp}	$\Delta g_{\parallel} = g_e - g_{\parallel}$	$\Delta g_{\perp} = g_e - g_{\perp}$	Δg_{\parallel}
						Δg_{\perp}
Ti^{3+} ($3d^1$)	ScPO_4	1.913 (1)	1.961 (1)	0.089	0.041	2.17
	LuPO_4	1.895 (1)	1.961 (1)	0.107	0.041	2.61
	YPO_4	1.885 (1)	1.9605 (5)	0.117	0.042	2.79
Zr^{3+} ($4d^1$) ^a	ScPO_4	1.871 (1)	1.936 (1)	0.131	0.066	1.98
	LuPO_4	1.844 (1)	1.933 (1)	0.158	0.069	2.29
	YPO_4	1.832 (1)	1.932 (1)	0.170	0.070	2.43
Hf^{3+} ($5d^1$) ^b	ScPO_4	1.550 (1)	1.773 (1)	0.452	0.229	1.97
	LuPO_4	1.461 (1)	1.757 (1)	0.541	0.245	2.21
	YPO_4	1.422 (1)	1.750 (1)	0.580	0.252	2.30

^aM. M. Abraham, L. A. Boatner, J. O. Ramey, and M. Rappaz, J. Chem. Phys. **81**, 5362 (1984).^bM. M. Abraham, L. A. Boatner, and J. O. Ramey, J. Chem. Phys. **83**, 2754 (1985).

signals due to Gd^{3+} and Zr^{3+} both of which were present as impurities unintentionally introduced in the crystal-growth process can be seen in the figure. The observed angular variation of the Ti^{3+} resonance spectrum in ScPO_4 again unequivocally established that the Ti^{3+} ion resides in a substitutional site in this host, and that there is only one Ti^{3+} site per unit cell. The spin-Hamiltonian parameters describing the Ti^{3+} EPR spectrum in ScPO_4 are tabulated in Tables I and II.

A single EPR line that was ultimately established as the spectrum of ^{47}Ti was observed in a single crystal of YPO_4 doped with naturally abundant Ti (5.51% ^{49}Ti , 7.28% ^{47}Ti , and 87.21% ^{47}Ti). Initially this spectrum could not be conclusively attributed to Ti^{3+} since the characteristic hyperfine pattern of the odd Ti isotopes was not detectable due to the low intensity of the hyperfine lines. Accordingly, YPO_4 crystals doped with isotopically enriched ^{47}Ti (94.55% ^{47}Ti , 0.19% ^{49}Ti , and 5.26% ^{47}Ti) were grown, and the associated EPR spectrum for $\text{H}||c$ is illustrated in Fig. 5. Six hyperfine lines due to the enriched ^{47}Ti isotope ($I = 5/2$) are seen flanking the ^{49}Ti central line. These transitions are labeled at the bottom of the figure. The EPR lines due to the ^{49}Ti isotope ($I = 7/2$) are too weak to be detected as a result of the isotopic enrichment. Additionally, a resonance line due to ^{91}Zr and a portion of the ^{91}Zr hyperfine structure can be seen in the figure. In order to determine the hyperfine parameters for the ^{49}Ti isotope, YPO_4 crystals doped with enriched ^{49}Ti (96.25% ^{49}Ti , 0.22% ^{47}Ti , 3.53% ^{47}Ti) were also grown, and the resulting EPR spectrum is shown in Fig. 6. This spectrum, recorded with the applied magnetic field parallel to the crystal c axis, exhibits the eight hyperfine lines characteristic of ^{49}Ti ($I = 7/2$). Additional EPR lines due to Zr^{3+} can be seen. With the magnetic field rotated from the c axis ($\theta = 0^\circ$) toward the a axis ($\theta = 90^\circ$) of the tetragonal YPO_4 crystal, the behavior of the Ti^{3+} resonance spectrum in YPO_4 is similar to that found for LuPO_4 and ScPO_4 (i.e., the titanium lines exhibit the axial symmetry characteristic of the local substitutional site and there is only one magnetic site per unit cell). The spin-Hamiltonian parameters determined for Ti^{3+} in YPO_4 are given in Tables I and II. For

comparison, Table I also lists the spectroscopic splitting parameters obtained previously for the Zr^{3+} ($4d^1$) and Hf^{3+} ($5d^1$) ions in these same hosts.

A free ion with a d^1 electronic configuration has a fivefold orbital degeneracy. The crystal field of the tetragonal orthophosphate hosts employed here can be considered as a superposition of an eightfold cubic crystal field with an additional tetragonal distortion. The cubic crystal field splits the fivefold orbital degeneracy of the free ion into a ground doublet level and an excited triplet level. With the additional tetragonal distortion, the ground orbital doublet is split into two orbital singlets. Either of these orbital singlets (which still retain twofold spin degeneracy) can be the ground state and the observed magnetic resonance spectrum is due to a transition between the two spin levels in the orbital singlet ground state. The spin-orbit interaction can admix a portion of the upper orbital triplet into the ground orbital singlet and change the spectroscopic splitting factors g_{\parallel} and g_{\perp} from the first-order free electron value $g_e = 2.00232$. Matrix elements of the spin-orbit coupling connect the ground state only with states of the upper triplet; therefore, the departure of the two g values from the free-electron value may be expressed in terms of the spin-orbit coupling constant and the energy separations between the ground singlet and one or the other of the two levels of the upper triplet. (The latter is split into a singlet and a doublet by the tetragonal distortion.)

TABLE II. Hyperfine parameters for Ti^{3+} at 77 K.

Host	$^{49}\text{A}_{\parallel} (I = 7/2)$ (G)	$^{49}\text{A}_{\perp} (I = 7/2)$ (G)	$^{47}\text{A}_{\parallel} (I = 5/2)$ (G)	$^{47}\text{A}_{\perp} (I = 5/2)$ (G)
ScPO_4	32.7 (1)	10.4 (2)
YPO_4	34.9 (1)	11.1 (2)	34.8 (1)	11.3 (2) ^a
LuPO_4	34.2 (2)	10.6 (2)

^aFor YPO_4 , the hyperfine values for both odd isotopes permit a calculation of the ratio of the magnetic moments for the two odd Ti isotopes. The value of $^{49}\mu/^{47}\mu = 1.4040$ compares well with the values of 1.4004 calculated using the data given by G. H. Fuller and V. W. Cohen, Nuclear Data Tables Sec. A **5**, 433 (1969).

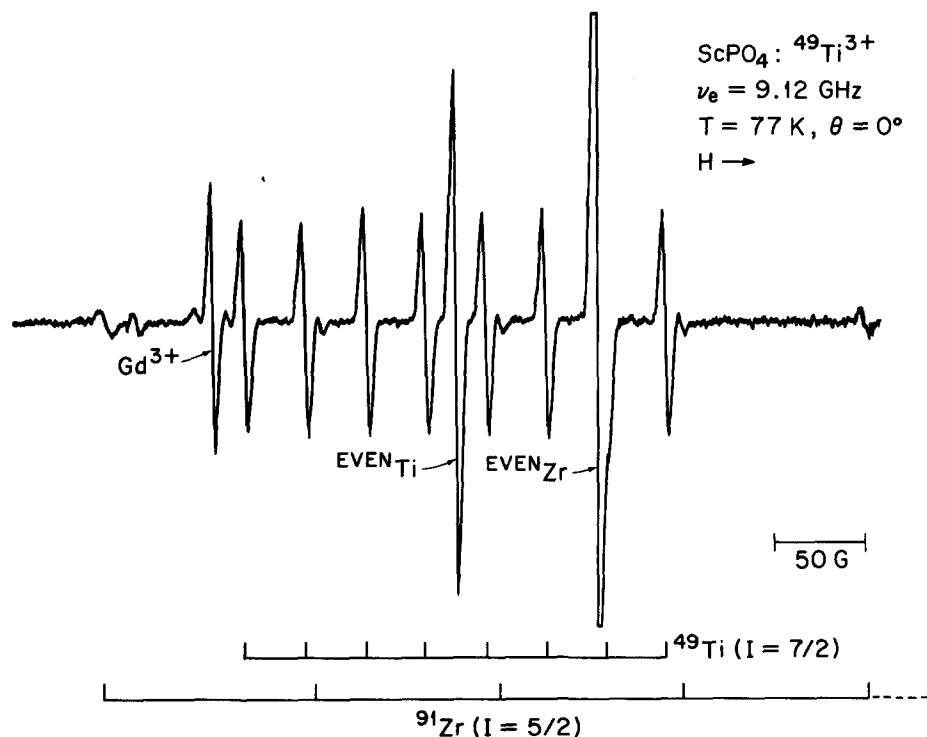


FIG. 3. EPR spectrum of isotopically enriched Ti³⁺ (enriched to 76.27% ⁴⁹Ti) at 77 K in a single crystal of ScPO₄. The first derivative spectrum, recorded with the applied magnetic field parallel to the fourfold symmetry *c* axis of the tetragonal host crystal, exhibits eight hyperfine lines due to the enriched ⁴⁹Ti isotope flanking the ^{even}Ti central line. In addition to the Ti³⁺ absorption lines, resonance lines due to Gd³⁺ and Zr³⁺ are also evident.

The spin Hamiltonian parameters listed in Tables I and II for Ti³⁺, as well as the previously reported parameters for Zr³⁺ and Hf³⁺ in the same three hosts, all have $g_\perp > g_\parallel$ and $A_\parallel > A_\perp$. This demonstrates that the orbital ground state is described by the symmetric wave function $[1/\sqrt{2}](|+2\rangle + |-2\rangle)$ which transforms as $(x^2 - y^2)$. Attempts to fit the experimental data for any of these *d*¹ ions to the theory of Abragam and Pryce²² in order to calculate the

energy separation between the orbital levels produced by the crystal field have been unsuccessful. Whatever the origin of the additional effects that must be taken into account in order to fit the experimental data, it is clear that coupling to other electronic levels is important. This is evidenced by the observation that the *g* and *A* values for the Ti³⁺ and Zr³⁺ ions which can be measured at room temperature are different than the values determined at 77 K. At room tempera-

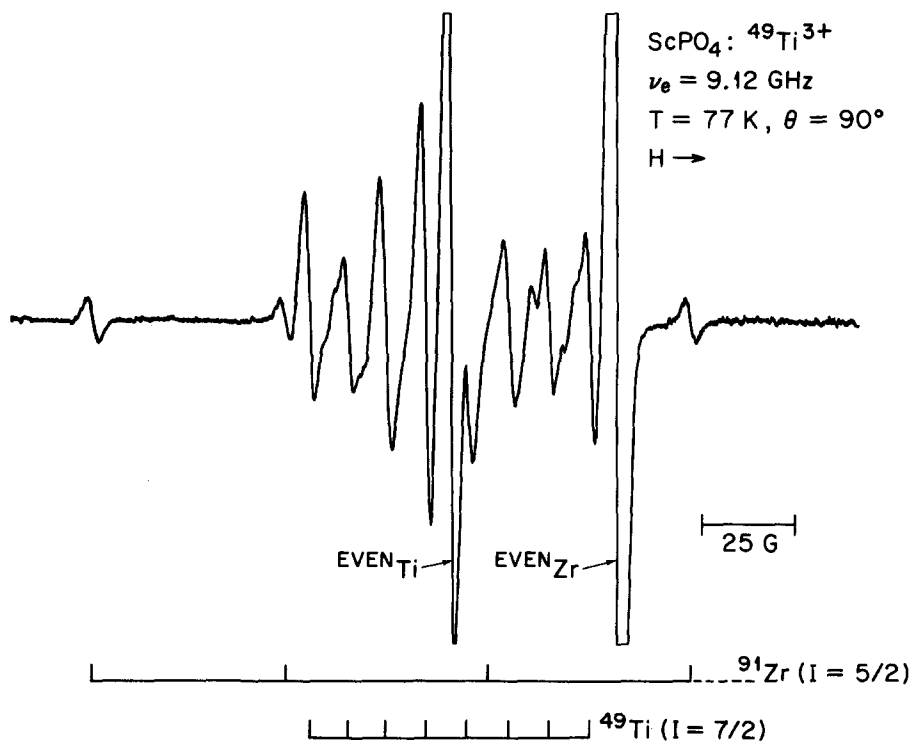


FIG. 4. First derivative EPR spectrum of isotopically enriched Ti³⁺ (enriched to 76.27% ⁴⁹Ti) at 77 K in a single crystal of ScPO₄, with the applied magnetic field perpendicular to the *c* axis of the crystal. The bar diagram below the spectrum labels the eight hyperfine lines of ⁴⁹Ti, the single line due to ^{even}Ti, a single line due to ^{even}Zr³⁺, and four of the six ⁹¹Zr ($I = 5/2$) hyperfine lines. The trivalent zirconium is present as an unintentional impurity, which originates in the crystal growth process.

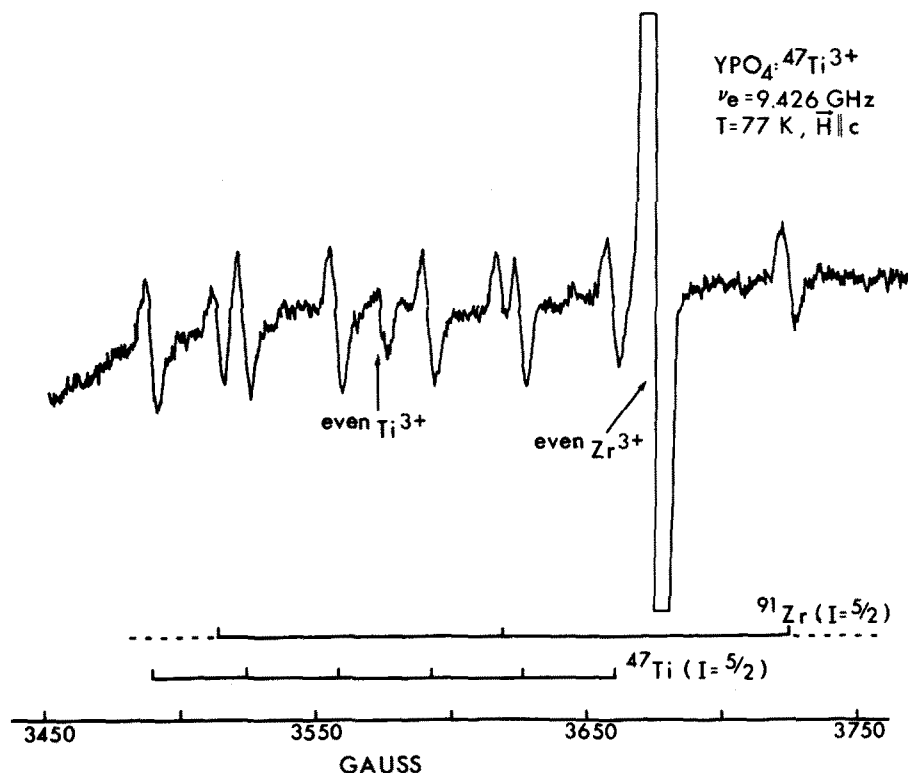


FIG. 5. EPR spectrum of isotopically enriched Ti³⁺ (enriched to 94.55% ⁴⁷Ti) at 77 K in a single crystal of YPO₄ with the applied magnetic field parallel to the *c* axis of the tetragonal crystal. The spectrum is shown as a first derivative of absorption. Six hyperfine lines due to the enriched ⁴⁷Ti isotope are seen flanking the ^{even}Ti central line and are labeled at the bottom of the figure. The signals of the ⁴⁹Ti isotope are too weak to be detected as a result of the isotopic enrichment. Additionally, a resonance line due to ^{even}Zr and a portion of the ⁹¹Zr hyperfine structure can be seen in the figure.

ture the departures of the *g* values from the free electron value (Δg_{\parallel} or Δg_{\perp}) are slightly larger for these two ions and the hyperfine values are slightly smaller than their respective values at 77 K.

It should also be noted that the Δg 's increase for each

trivalent *d*¹ ion in the order of the series of hosts: ScPO₄ to LuPO₄ to YPO₄, and that they also increase as the principal quantum number goes from 3 to 5. The trend of increasing Δg 's as the host is varied as indicated implies that the strength of the crystal-field interaction with the *d* electron in

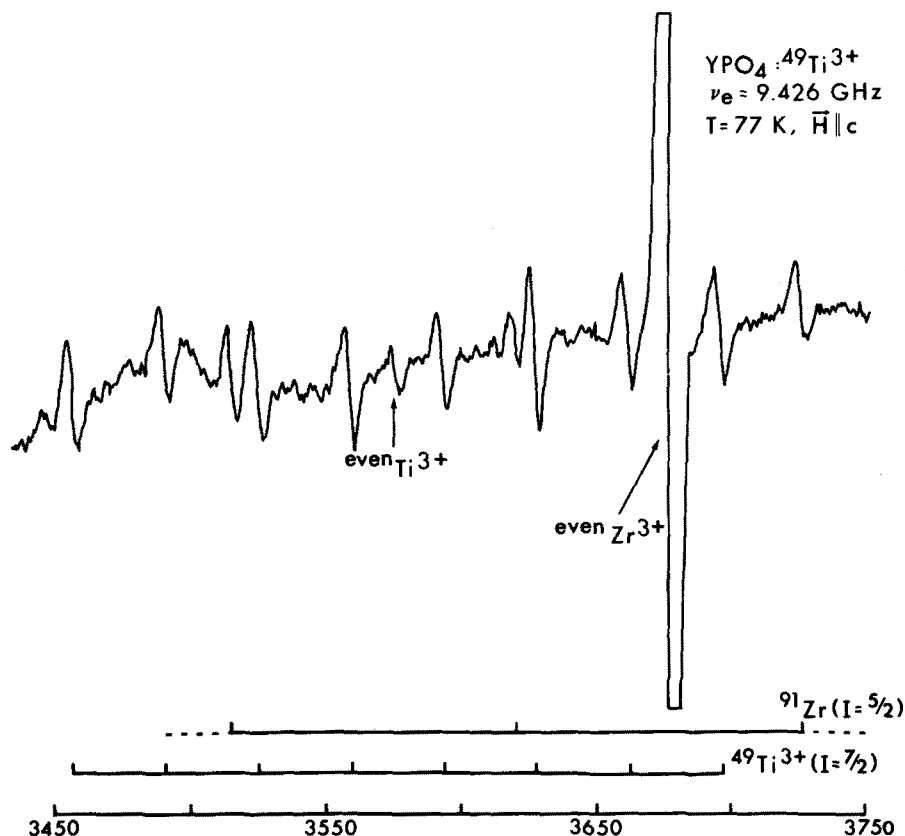


FIG. 6. First derivative EPR spectrum of isotopically enriched Ti³⁺ (enriched to 96.25% ⁴⁹Ti) at 77 K in a single crystal of YPO₄. The spectrum, recorded with the applied magnetic field parallel to the crystal *c* axis, exhibits the eight hyperfine lines of ⁴⁹Ti which are labeled by the bar diagram below the trace. Absorption lines due to Zr³⁺ are also present.

the ScPO_4 , LuPO_4 , and YPO_4 hosts is in descending order of magnitude. A similar descending order of magnitude for the crystal-field interaction has been observed for the d^5 configuration ion Fe^{3+} in these same hosts.⁷ On the other hand, the crystal-field interaction for the f^7 configuration ion Gd^{3+} in these identical hosts is quite different and the strength of the crystal-field interaction for Gd^{3+} descends in going from YPO_4 to LuPO_4 to ScPO_4 .⁶ Certainly this reversal of field strength for the d^5 and f^7 ions is not unexpected since the exact mechanism responsible for the splitting of an S state by the crystal field is at present unknown.

While the literature dealing with the ground state spectroscopic properties of d^1 -configuration ions in tetragonal sites in host single crystals is not extensive, there are nevertheless a number of notable examples in which systems of this type have been studied previously. These include investigations of W^{5+} in CaWO_4 ,²³ Cr^{5+} in YPO_4 and YVO_4 ,²⁴ V^{4+} in AlPO_4 ,^{25,26} ZrSiO_4 ,^{27,28} HfSiO_4 ,²⁸ ThSiO_4 ,²⁸ ThGeO_4 ,²⁸ and GeO_2 ,^{29,30} Mo^{5+} in YVO_4 ,³¹ and Nb^{4+} in ZrSiO_4 .³² This earlier work has, in general, been characterized by the same inability to account for the observed g values by means of second order crystal-field admixtures to nearby excited states that we have encountered in our investigations of the trivalent d^1 ions Ti^{3+} , Hf^{3+} , and Zr^{3+} . Although previous workers have proposed a variety of possible mechanisms in order to explain the earlier experimental results, a definitive solution has not been forthcoming. In the present case, results are now available for a series of three isovalent d^1 configuration ions in a series of three isostructural tetragonal-symmetry hosts. Hopefully, the trends evidenced by the g values determined for these nine different systems will provide an indication for the direction of future theoretical efforts to account for the important spectroscopic properties of single d -electron systems.

ACKNOWLEDGMENTS

The authors acknowledge with thanks the contributions of J. O. Ramey to the crystal growth and Lazelle Tyler to the preparation of the manuscript.

- ¹L. A. Boatner, G. W. Beall, M. M. Abraham, C. B. Finch, P. G. Huray, and M. Rappaz, *Scientific Basis for Nuclear Waste Management*, edited by C. J. Northrup (Plenum, New York, 1980), Vol. II, p. 289.
- ²M. M. Abraham, L. A. Boatner, G. W. Beall, C. B. Finch, R. J. Floran, P. G. Huray, and M. Rappaz, in *Alternate Nuclear Waste Forms and Interactions in Geologic Media*, CONF-8005107, edited by L. A. Boatner and G. C. Battle, Jr. (USDOE, Washington, D. C., 1981), p. 144.

- ³L. A. Boatner, G. W. Beall, M. M. Abraham, C. B. Finch, R. J. Floran, P. G. Huray, and M. Rappaz, *Management of Alpha-Contaminated Wastes*, IAEA-SM 246/73 (IAEA, Vienna, 1981), p. 411.
- ⁴M. M. Abraham, L. A. Boatner, and M. Rappaz, *Phys. Rev. Lett.* **45**, 839 (1980).
- ⁵M. Rappaz, M. M. Abraham, J. O. Ramey, and L. A. Boatner, *Phys. Rev. B* **23**, 1012 (1981).
- ⁶M. Rappaz, L. A. Boatner, and M. M. Abraham, *J. Chem. Phys.* **73**, 1095 (1980).
- ⁷M. Rappaz, J. O. Ramey, L. A. Boatner, and M. M. Abraham, *J. Chem. Phys.* **76**, 40 (1982).
- ⁸M. M. Abraham, L. A. Boatner, J. O. Ramey, and M. Rappaz, *J. Chem. Phys.* **78**, 3 (1983).
- ⁹M. M. Abraham and L. A. Boatner, *Phys. Rev. B* **26**, 1434 (1982).
- ¹⁰J. L. Boldú O., E. Muñoz P., M. M. Abraham, and L. A. Boatner, *J. Chem. Phys.* **83**, 6113 (1985).
- ¹¹M. M. Abraham, L. A. Boatner, J. O. Ramey, and M. Rappaz, *J. Chem. Phys.* **81**, 5362 (1984).
- ¹²M. M. Abraham, L. A. Boatner, and J. O. Ramey, *J. Chem. Phys.* **83**, 2754 (1985).
- ¹³W. O. Milligan, D. F. Mullica, G. W. Beall, and L. A. Boatner, *Inorg. Chim. Acta* **60**, 39 (1982).
- ¹⁴W. O. Milligan, D. F. Mullica, G. W. Beall, and L. A. Boatner, *Inorg. Chim. Acta* **70**, 133 (1983).
- ¹⁵W. O. Milligan, D. F. Mullica, G. W. Beall, and L. A. Boatner, *Acta Crystallogr. Sect. C* **39**, 23 (1983).
- ¹⁶G. M. Begun, G. W. Beall, L. A. Boatner, and W. T. Gregor, *J. Raman Spectrosc.* **11**, 173 (1981).
- ¹⁷T. Hayhurst, S. Shalimoff, N. Edelstein, L. A. Boatner, and M. M. Abraham, *J. Chem. Phys.* **74**, 5449 (1981).
- ¹⁸T. Hayhurst, G. Shalimoff, J. G. Conway, N. Edelstein, L. A. Boatner, and M. M. Abraham, *J. Chem. Phys.* **76**, 3960 (1982).
- ¹⁹P. C. Becker, T. Hayhurst, G. Shalimoff, J. G. Conway, L. A. Boatner, and M. M. Abraham, *J. Chem. Phys.* **81**, 2872 (1984).
- ²⁰P. C. Becker, N. Edelstein, G. M. Williams, J. J. Bucher, R. E. Russo, J. A. Konigstein, L. A. Boatner, and M. M. Abraham, *Phys. Rev. B* **31**, 8102 (1985).
- ²¹B. C. Sales, C. W. White, and L. A. Boatner, *Nucl. Chem. Waste Management* **4**, 281 (1983).
- ²²A. Abragam and M. H. L. Pryce, *Proc. R. Soc. London Ser. A* **205**, 135 (1951); **206**, 164 (1951); B. Bleaney, K. D. Bowers, and M. H. L. Pryce, *ibid.* **228**, 166 (1955), and references therein.
- ²³V. P. Solntsev and M. Ya. Shcherbakova, *Zh. Strukt. Khim.* **12**, 397 (1971) [*Eng. Trans. J. Struct. Chem.* **12**, 369 (1971)].
- ²⁴M. Greenblatt, J. H. Pifer, B. R. McGarvey, and B. M. Wanklyn, *J. Chem. Phys.* **74**, 6014 (1981).
- ²⁵R. S. de Biasi, *J. Phys. C* **13**, 6235 (1980).
- ²⁶R. S. de Biasi, *J. Phys. C* **15**, 1297 (1982).
- ²⁷D. Ball and B. M. Wanklyn, *Phys. Status Solidi* **36**, 307 (1976).
- ²⁸S. Di Gregorio, M. Greenblatt, J. H. Pifer, and M. D. Sturge, *J. Chem. Phys.* **76**, 2931 (1982).
- ²⁹David P. Madaci, R. H. Bartram, and O. R. Gilliam, *Phys. Rev. B* **7**, 1817 (1973).
- ³⁰D. P. Madaci and O. R. Gilliam, *Phys. Lett. A* **41**, 63 (1972).
- ³¹J. H. Pifer, S. Ziemiński, M. Greenblatt, and B. M. Wanklyn, *J. Solid State Chem.* **45**, 93 (1982).
- ³²V. M. Vinokurov, M. M. Zaripov, V. G. Stepanov, G. K. Chirkin, and L. Ya. Shekun, *Fiz. Tverd. Tela* **5**, 2034 (1963) [*Eng. Trans. Sov. Phys. Solid State* **5**, 1487 (1963)].